

Nonequilibrium Theory for Adaptive Systems in Varying Environments

Ying-Jen Yang,^{1,*} Charles D. Kocher,^{2,†} and Ken A. Dill^{1,2,3}

¹*Laufer Center for Physical and Quantitative Biology, Stony Brook University, Stony Brook, NY 11794*

²*Department of Physics and Astronomy, Stony Brook University, Stony Brook, NY 11794*

³*Department of Chemistry, Stony Brook University, Stony Brook, NY 11794*

Biological organisms are adaptive, able to function in unpredictably changing environments. Drawing on recent nonequilibrium physics, we show that in adaptation, fitness has two components parameterized by observable coordinates: a static *Generalism* component characterized by state distributions, and a dynamic *Tracking* component sustained by nonequilibrium fluxes. Our findings: (1) *General Theory*: We prove that tracking gain scales strictly with environmental variability and switching time-scales; near-static or fast-switching environments are not worth tracking. (2) *Optimal Strategies*: We explain optimal bet-hedging and phenotypic memory as the interplay between these components. (3) *Control*: We demonstrate, with an example, how to suppress pathogens by independently attacking their Generalism robustness (via environmental time fractions) and Tracking capabilities (via environmental switching speed). This work provides a physical framework for understanding and controlling adaptivity.

We seek design principles for the optimization and control of adaptive dynamics. We consider the dynamics of a system, like a biological organism, that has some *fitness* based on its ability to track dynamical change in its environment. The ability to adapt to varying environments is fundamental for biological success [1–3], prompting extensive theoretical [4–8] and experimental [9–12] investigation into organisms’ adaptive strategies. These strategies can be broadly classified into two types: (1) *Tracking* strategies, where the organism senses the environment and shifts its phenotype or internal state according to the current [13, 14] or anticipated [15–20] conditions, and (2) non-tracking strategies (or “*Generalism*,” in the broad sense), including the “pure” generalist (a single robust phenotype that does not switch) [21, 22] and stochastic bet-hedging (random, environment-independent switching between phenotypes) [23–27]. Intuitively, Generalism is akin to wearing a versatile jacket suitable for most weather, while Tracking is the extra gain from actively changing outfits to match the specific environment.

Previous work has analyzed and computed optimal strategies for given environmental scenarios [4, 28–31] and revealed (phase) transitions to distinct optimal states in different environmental settings [8, 32–34]. However, merely identifying the optimal strategy offers limited guidance on the underlying mechanisms and how a suboptimal organism can adjust to improve long-term growth. Knowing the location of a summit does not inherently reveal the trail to reach it. To address this gap, we need a navigational map that identifies the distinct physical components of the “fitness elevation,” thereby revealing axes for optimization and control.

In this work, we demonstrate that the long-term growth rate of a population adapting to a varying environment can be decomposed into the exact sum of contributions from the two distinct strategies: (1) a static Generalism term, derived

from the overlap between system (π_x) and environmental (π_E) state occupancies, and (2) a dynamic Tracking term, strictly proportional to the nonequilibrium probability flux J scaled by the environmental switching time scale \mathcal{T}_{env} ,

$$\text{Fitness} = \underbrace{\text{Generalism}(\pi_E, \pi_x)}_{\text{Static / Equilibrium}} + \underbrace{\text{Tracking}(\mathcal{T}_{\text{env}}, J)}_{\text{Dynamic / Nonequilibrium}}. \quad (1)$$

Drawing on landscape-flux theory [35–37] and the recent Caliber Force Theory [38], we identify π_x and J as the **observable coordinates** for adaptive dynamics. Just as latitude and longitude are needed to navigate a map, Generalism (π_x) and Tracking (J) are the orthogonal axes needed to navigate fitness. This coordinate geometry reveals their separate tunability and the internal degeneracy in fitness (Example 1).

The utility of this coordinate map lies in the distinct physical nature of its components. **First**, because Generalism is characterized by the static distribution π_x and Tracking from the dynamic flux J , they exhibit different sensitivities to system parameters, allowing us to explain optimal adaptive strategies as the interplay of these two axes, such as bet-hedging [4, 7] (Example 2) and phenotypic memory [33] (Example 3). **Second**, the two components are governed by different environmental statistics: Generalism depends on environmental bias (π_E), while Tracking is limited by the environmental switching time scale (\mathcal{T}_{env}). This separation suggests targeted control strategies, such as optimizing drug regimens to suppress pathogens by independently attacking their Generalism versus Tracking capabilities (Example 4). **Third**, this decomposition provides a practical shortcut for gauging the relative contributions of each strategy. Without the need to measure the fluxes (J), the Tracking contribution can be computed from the total growth rate by subtracting the measurable Generalism term. By mapping fitness onto these physical coordinates, we offer a framework to design adaptive strategies and inform the rational control of systems adapting to varying environments.

* ying-jen.yang@stonybrook.edu

† Now at Memorial Sloan Kettering Cancer Center, New York, NY 10065

THEORETICAL FRAMEWORK FOR FITNESS PARSING

We first quantify fitness. For an adaptive system reaching a statistical steady state under a varying environment,¹ fitness is naturally quantified as the Long-Term logarithmic Growth Rate of the population (LTGR). By time additivity and ergodicity, this growth rate is exactly equal to the long-term average of the per capita growth rate $g(E, x)$:

$$\text{Fitness} = \lim_{t \rightarrow \infty} \frac{1}{t} \ln \frac{N(t)}{N(0)} = \sum_{E,x} \pi_{E,x} g(E, x) \quad (2)$$

Here, $\pi_{E,x}$ represents the joint probability between the system's state x and the environment's state E . The state variables (E, x) encode the time dependency of g : $g[E(t), x(t)] = \dot{N}(t)/N(t)$.

Environments with low variability are not worth tracking. We analyze how much of the statistical alignment $\pi_{E,x}$ (or *synchrony*) is contributed from an independent baseline $\pi_x \pi_E$ (Generalism) and how much is from the additional gain from Tracking. By expressing the joint probability using marginal distributions (π_E and π_x) and conditional distributions ($\pi_{x|E} = \pi_{E,x}/\pi_E$), a general parsing of the system-environment synchrony can be derived with a simple rewriting (Appendix A1 [43]):

$$\pi_{E,x} = \pi_E \pi_x + \sum_{E'(\neq E)} \pi_E \pi_{E'} (\pi_{x|E} - \pi_{x|E'}). \quad (3)$$

The first term on the right represents a baseline that can be matched with a system independent of the environment (Generalism), whereas the second term represents how much a state is preferred in environment E opposed to other environments E' (Tracking). This latter term is the additional contribution from system-environment coupling.

Eq. (3) immediately offers an insight into environmental statistics: the Tracking term scales with the ‘‘variability of the environment’’ $\pi_E \pi_{E'}$. If the environment is highly biased toward one state (i.e., one $\pi_E \rightarrow 1$ and others $\rightarrow 0$), the Tracking term diminishes. Thus, environments that are predominantly static (low variability) are not worth tracking.

Rapidly changing environments are not worth tracking.

To relate Tracking to nonequilibrium flux, we suppose that the environment-system pair follows a continuous-time Markov jump process. In each infinitesimal time step dt , only two types of transitions are possible: either the system changes $(E, x) \mapsto (E, x')$ with rates $R_{xx'}(E)$ or the environment changes $(E, x) \mapsto (E', x)$ with rates $R_{E'E'}(x)$. A simultaneous change is higher order, $\mathcal{O}(dt^2)$, negligible in

continuous time. This is known as a *bipartite* process [44–46].

At the steady state, the total outward net flux from any joint state (E, x) must be zero:

$$0 = \sum_{E'(\neq E)} \pi_{E,x} R_{EE'}(x) - \pi_{E',x} R_{E'E}(x) + \sum_{x'(\neq x)} \pi_{E,x} R_{xx'}(E) - \pi_{E,x'} R_{x'x}(E). \quad (4)$$

For a given system state x , we assume that the *environment evolves on its own* (i.e. $R_{EE'}(x) = R_{EE'}$ are independent of the system's state) and vectorize Eq. (4) across all possible environmental states E :

$$\mathbf{0} = -\pi_{\text{joint}} \mathbf{R}_{\text{env}} + \text{div}_{\text{sys}} \mathbf{J} \quad (5)$$

where $\pi_{\text{joint}} = (\pi_{E_1,x}, \dots, \pi_{E_N,x})$ is a row vector of the joint probability under different environments, \mathbf{R}_{env} is the transition rate matrix of the environment, and $\text{div}_{\text{sys}} \mathbf{J}$ is the row vector of system-wise net flux divergences (for each E , spreading out to all $x'(\neq x)$ from a fixed x). See Appendix A2 for details [43]. Since $\pi_{\text{env}} = (\pi_{E_1}, \dots, \pi_{E_N})$ is the steady-state distribution of the environment, satisfying $\pi_{\text{env}} \mathbf{R}_{\text{env}} = \mathbf{0}$, we can expand π_{joint} around the decoupled baseline $\pi_{\text{env}} \pi_x$. ‘‘Inverting’’ \mathbf{R}_{env} yields:

$$\pi_{\text{joint}} = \pi_{\text{env}} \pi_x + (\text{div}_{\text{sys}} \mathbf{J})(\tilde{\mathbf{R}}_{\text{env}}^{-1}) \quad (6)$$

where $\tilde{\mathbf{R}}_{\text{env}}^{-1}$ is the Drazin inverse (or generalized inverse) of the environmental transition rate matrix \mathbf{R}_{env} . This inverse matrix captures the relaxation time of the environment. It is constructed via spectral decomposition $\tilde{\mathbf{R}}_{\text{env}}^{-1} = \sum_{\lambda_k \neq 0} \lambda_k^{-1} \mathbf{v}_k^T \mathbf{u}_k$ where λ_k are the eigenvalues of \mathbf{R}_{env} with corresponding left (\mathbf{u}_k) and right (\mathbf{v}_k^T) eigenvectors. The reciprocals of these eigenvalues are proportional to the environmental time scales \mathcal{T}_{env} . Thus, under fast environmental switching ($\mathcal{T}_{\text{env}} \rightarrow 0$), the Tracking contribution vanishes.

This result mirrors the equilibrium-nonequilibrium splitting of dynamics in stochastic thermodynamics [47–49]. By demonstrating that Tracking necessarily involves nonequilibrium fluxes, our parsing clarifies the fundamental connection between time irreversibility and adaptive dynamics [41, 42, 50–53]. However, viewed through the lens of landscape-flux theory [35–37] and the recent Caliber Force Theory [38], Eq. (6) reveals a deeper structure: Generalism (π_x) and Tracking (J) constitute thermodynamics-like **observable coordinates** for adaptive dynamics and are distinct degrees of freedom that can be **tuned independently**. Moreover, this coordinate mapping highlights a **design degeneracy** in adaptive dynamics allowing bidirectional transitions: since fitness is fully determined by Generalism π and Tracking J , the remaining degrees of freedom—the noise strength in diffusion [35–37] or the ‘‘traffic’’ (sum of both way fluxes) in Markov jumps [38, 54]—can be varied without altering fitness, provided that (π_x, J) remain constant (Example 1).

¹ The steady state has been called the ‘‘red queen’’ scenario [39–42], a situation where a species constantly adapts to a changing environment. This term comes from Alice in Wonderland; it is a race in which you must always keep running as fast as you can just to ‘‘stay in place’’ (stay alive).

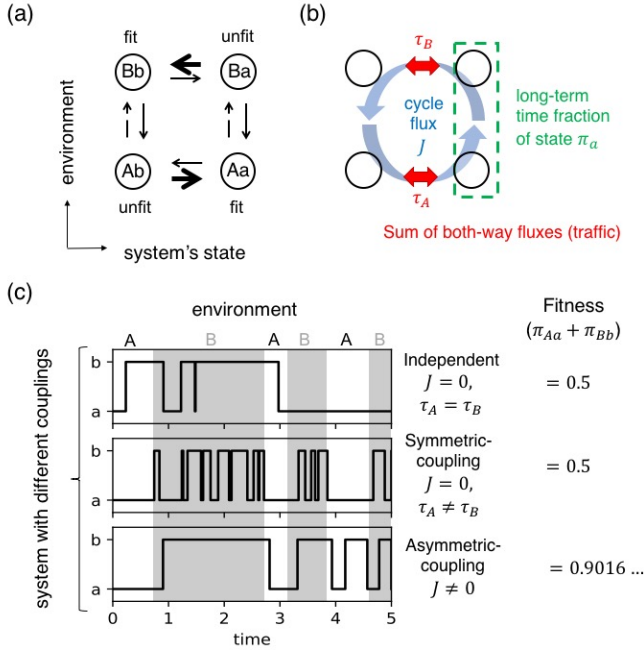


FIG. 1. **The state space, observables, and types of system-environment coupling of a simple adapting individual.** (a) The total state space of the two-state system $\{a, b\}$ under a Markov environmental switch $\{A, B\}$. Vertical arrows are environmental transitions and horizontal arrows are system transitions. (b) Four statistical observables that fully parameterize the system's dynamics. π_a is the long-term time fraction that the system is in a regardless of the environmental state. Traffic τ_E are the sum of fluxes in both direction under environment E . J is the net cycle flux. (c) Three types of system-environment coupling classified by the observables. Net flux J is needed to track the environment and outperform an independent switch in the synchronization task. Fitness values shown on the right are the long-term time fraction of being at the synchronized (fit) states. Parameters used in (c) are as follows: $R_{AB} = R_{BA} = 1$, $g_a(A) = g_b(B) = 1$ and $g_a(B) = g_b(A) = 0$ for all three cases. $R_{ab}(E) = R_{ba}(E) = 1$, $E = A$ or B , for the independent case; $R_{ab}(A) = R_{ba}(A) = 0.1$, $R_{ab}(B) = R_{ba}(B) = 10$ for the symmetric-coupling case; $R_{ab}(A) = 0.2$, $R_{ba}(A) = 10$, $R_{ab}(B) = 10$, $R_{ba}(B) = 0.2$ for the asymmetric-coupling case.

EXAMPLE 1: ADAPTING TO A 2-STATE MARKOV SWITCHING ENVIRONMENT

Here, we illustrate our framework with a minimal model. Suppose an individual in the population can take either of two phenotypic states $\phi \in \{a, b\}$ under a two-state switching environment $E \in \{A, B\}$. State a is more fit in environment A , and state b is more fit in B . For a Markov switching environment and system, the joint state space is a square with four nodes and four edges (Fig. 1a). This model can describe, for example, a single chemo-sensing receptor in *E. coli* [55], or—our focus here—phenotype-switching individuals in a population under the slow growth limit.

Slow Growth Approximation. Strictly speaking, the state

of an adaptive population is the vector $\mathbf{x} = (N_a, N_b)$, which determines the instantaneous growth rate of the total population $N(t) = N_a(t) + N_b(t)$. However, the population composition is dynamically skewed by the interplay of switching and differential growth (i.e., fitter phenotypes accumulate faster and skew the distribution). While we will address this full population dynamics in later examples, here we simplify the problem by focusing on the individual phenotype $\phi \in \{a, b\}$ and the phenotype switching. Let g_ϕ denote the growth rate and $R_{\phi\phi'}$ the switching rates. We consider the limit where individual replication is much slower than switching ($g_\phi \ll R_{\phi\phi'}$). Under this time-scale separation, the relevant state description reduces from the population counts \mathbf{x} to the individual phenotype ϕ , as the population composition effectively relaxes to the quasi-static switching distribution $\pi_{E,\phi}$ before differential growth can significantly distort it. This allows us to approximate the population fitness simply as the expected replication rate of a single stochastic individual in this example:

$$\text{LTGR} = \lim_{t \rightarrow \infty} \frac{1}{t} \ln \frac{N(t)}{N(0)} \approx \sum_{E,\phi} \pi_{E,\phi} g_\phi(E). \quad (7)$$

This approximation effectively transforms the problem from solving coupled population differential equations into a simpler statistical task of computing averages over the single-particle stationary distribution.

Fitness Decomposition. We now apply the general decomposition derived in the Theory section (Eqs. 3 and 6) to this system. The Generalism term can be obtained by simply replacing $\pi_{E,\phi}$ with $\pi_E \pi_\phi$ in Eq. (7), leading to $\pi_a \bar{g}_a + \pi_b \bar{g}_b$ where $\bar{g}_\phi = \pi_A g_\phi(A) + \pi_B g_\phi(B)$ is the environment-averaged growth rate. The Tracking term requires the Drazin inverse of the environmental transition matrix. For a 2-state environment, the transition matrix has only one non-zero eigenvalue $\lambda = -(R_{AB} + R_{BA})$, and the Drazin inverse is simply the inverse of this relaxation rate multiplied by the outer product of its eigenvectors. With details shown in Appendix B1 [43], combining Eqs. (6) and (7) yields:

$$\text{LTGR} = \underbrace{\pi_a \bar{g}_a + \pi_b \bar{g}_b}_{\text{Generalism}} + \underbrace{[\pi_A \pi_B \bar{T}]}_{\text{Tracking}} J \Delta_g \quad (8)$$

where $\bar{T} = R_{AB}^{-1} + R_{BA}^{-1}$ is the average environmental cycle period and $\Delta_g = [g_a(A) - g_b(A)] + [g_b(B) - g_a(B)]$ is the growth advantage of being in the correct state. This confirms our general theory: Tracking gain is proportional to the product of Environmental Variability ($\pi_A \pi_B$), Environmental Time Scale (\bar{T}), and the system's Nonequilibrium Flux (J).

Fitness Degeneracy. While Eq. (8) shows that fitness is determined entirely by π_a and J (given a fixed environment), these two coordinates are insufficient to fully describe adaptive dynamics. The system has four independent transition rates ($R_{ab}(A), R_{ba}(A), R_{ab}(B), R_{ba}(B)$), and thus requires four statistical observables for a complete parameterization. As illustrated in Fig. 1(b), the complete set are:

1. The total occupancy π_a (Generalism coordinate).
2. The net cycle flux J (Tracking coordinate).
3. Two “traffic” terms τ_A and τ_B , representing the sum of bidirectional fluxes in each environment, $\tau_E = \pi_{E,a}R_{ab}(E) + \pi_{E,b}R_{ba}(E)$ [38, 54].

These observable coordinates parameterize the transition rates $R_{xx'}(E) = (\tau_E \pm J)/(2\pi_{Ex})$, and this dimension accounting reveals a fundamental fitness degeneracy. The “traffic” difference $|\tau_A - \tau_B|$ corresponds to a symmetric coupling with the environment (e.g., the system switches faster in A than in B in *both* directions). While such symmetric coupling indicates that the system “senses” the environment, Eq. (8) shows it contributes nothing to fitness. Only the asymmetric, nonequilibrium coupling—manifested as non-zero flux J —enables the system to track and outperform an independent generalist (Fig. 1c).

The traffic terms τ_E serve only as kinetic constraints, limiting the maximum possible Tracking flux but not determining the direction of adaptation itself. This is because the amplitude of net flux on each edge $|J_{ij}| = |p_{ij} - p_{ji}|$ —where p_{ij} is the one way flux from i to j —can not surpass the traffic $\tau_{ij} = p_{ij} + p_{ji}$. This dynamical efficiency is exactly what the steady-state “entropy production” in stochastic thermodynamics [47–49], $\sum_{i < j} J_{ij} \ln[(\tau_{ij} + J_{ij})/(\tau_{ij} - J_{ij})]$ measures. See [38] for more discussions.

This example illustrates, in the simplest setting, the two implications of mapping fitness onto observable coordinates: separate tunability (Generalism π and Tracking J) and fitness degeneracy (traffic τ).

EXAMPLE 2: ACHIEVING OPTIMAL BET-HEDGING

We now go beyond the slow-growth limit in Example 1 to consider a large phenotype-switching population where individuals can reproduce, die, or switch phenotype under a Markov switching environment, as illustrated in Fig. 2(a). Commonly used to model phenotypic switching in microbes like *E. coli* [4, 33] or yeast [7] (or species reproducing with mutation; see Appendix C2 [43]), these dynamics are described by the following ODEs:

$$\frac{dN_a}{dt} = g_a(E)N_a - w_{ab}(E)N_a + w_{ba}(E)N_b, \quad (9a)$$

$$\frac{dN_b}{dt} = g_b(E)N_b + w_{ab}(E)N_a - w_{ba}(E)N_b, \quad (9b)$$

where $g_x = r_x - d_x$ is the net growth rate of type x with reproduction rate r_x and death rate d_x , which we presume to be constant and independent of the population size. In this deterministic limit, the adaptive dynamics flow without diffusive backtracking. Thus, unlike the discrete Example 1, the additional “traffic” variables are not needed (they equal to net fluxes for one-way flows), and the system exhibits no fitness degeneracy. We note, however, that the traffic

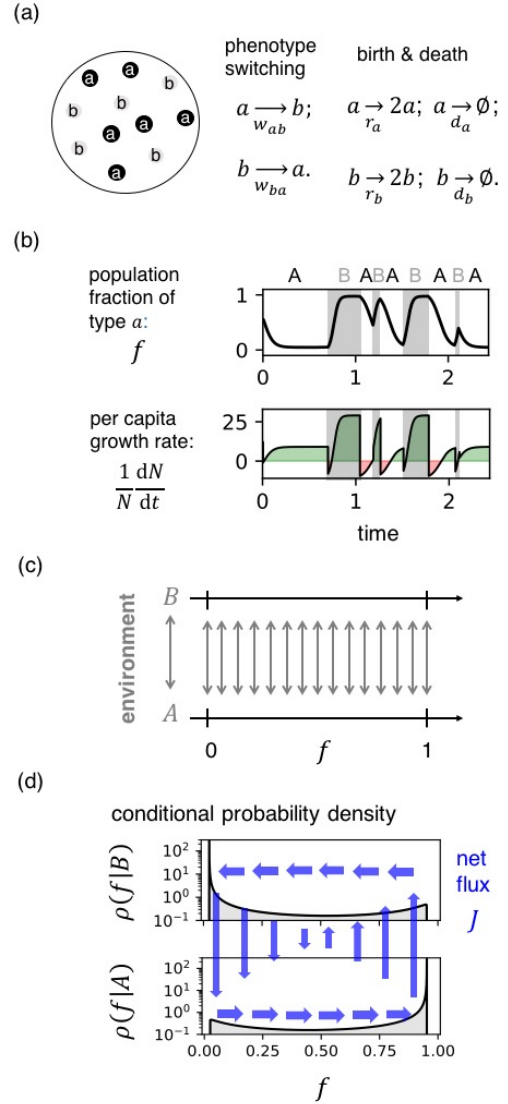


FIG. 2. The dynamics and total state space for a phenotype-switching population. (a) We consider the population dynamics of two-state individuals with Poisson birth-death and switching. (b) The population type fraction (of a) tracks the environmental changes and determines the instantaneous per capita growth rate. (c) The system-environment total state space consists of two line segments $f \in [0, 1]$, one for each environment A and B . The population can jump between the two segments at any f . (d) The (cyclic) net flux over the total state space leads to the long-term conditional probability density $\rho(f|E)$, forming a flux-tracking relation for population dynamics. Parameters used in (b) and (d) are: $R_{AB} = 2$, $R_{BA} = 1$, $g_a(A) = 30$, $g_b(B) = 10$, $g_a(B) = g_b(A) = -10$, and $w_{ab}(E) = w_{ba}(E) = 1$.

variables (and the associated degeneracy) would reappear if one analyzes the Poissonian stochastic dynamics before the large population limit—a level of detail of future interests but not required for the results derived here.

To extract the physical drivers of adaptation, it is standard to rewrite these equations in terms of more informative variables.

Denoting the total population $N = N_a + N_b$ and the population fraction of the a phenotype $f = N_a/N$, these ODEs become

$$\frac{df}{dt} = f(1-f)\Delta_{ab} + (f_w - f)\sigma_w, \quad (10a)$$

$$\frac{dN}{dt} = [g_a f + g_b(1-f)]N. \quad (10b)$$

where $\sigma_w = w_{ab} + w_{ba}$ is the sum of the switching rates, $f_w = w_{ba}/\sigma_w$ is the steady-state phenotype fraction if there's no growth (or death), and $\Delta_{ab} = g_a - g_b$ is the growth rate difference, also known as the selection coefficient. All these parameters depend on the environment. The rewriting shows that switching drives the type fraction f toward f_w with rate σ_w whereas natural selection, via the other term of df/dt , aims to fixate f toward 0 or 1 with a rate $|\Delta_{ab}|$. The overall dynamics is a balance of the two. Most importantly, it shows that the type fraction f is the sensing dimension that tracks the environmental changes, whereas the N dynamics in Eq. (10b) converts f into the per capita growth rate as the population's average fitness. See Fig. 2(b) for an example trajectory.

Fitness parsing for adaptive population: We now derive the fitness parsing for this deterministic adaptive system. First, observing that the per capita growth rate of N in Eq. (10b) is linear in f , the Long-Term Growth Rate (LTGR) is simply the time-average of the per capita growth rate. This average can be expressed as a summation of conditional averages (Appendix A4 of SM [43]):

$$\text{LTGR} = \lim_{t \rightarrow \infty} \frac{1}{t} \ln \frac{N(t)}{N(0)} \quad (11a)$$

$$= \sum_{\mathcal{E}} \pi_{\mathcal{E}} [g_a(\mathcal{E})\langle f|\mathcal{E} \rangle + g_b(\mathcal{E})(1 - \langle f|\mathcal{E} \rangle)] \quad (11b)$$

where $\pi_{\mathcal{E}}$ is the long-term occupancy of environment \mathcal{E} and

$$\langle f|\mathcal{E} \rangle = \lim_{t \rightarrow \infty} \frac{\int_0^t f(s) \delta_{E(s), \mathcal{E}} ds}{\text{total time in } \mathcal{E}} \quad (12)$$

is the conditional long-term empirical average of f under environment \mathcal{E} . The term $\delta_{E(s), \mathcal{E}}$ within the integral is a Kronecker delta function, which collapses the integral so that it is only taken over times when the system is in environment \mathcal{E} . For Markov switching environments, the conditional average $\langle f|\mathcal{E} \rangle$ has an analytical expression that can be computed numerically without ensemble simulations [29–31], which we've used throughout the paper.

Algebraically rearranging Eq. (11b) allows us to separate the environment-averaged contribution (Generalism) from the environment-dependent difference (Tracking):

$$\text{LTGR} = \underbrace{\langle f \rangle \bar{g}_a + \langle 1-f \rangle \bar{g}_b}_{\text{Generalism}} + \underbrace{\pi_A \pi_B [\langle f|A \rangle - \langle f|B \rangle]}_{\text{Tracking}} \Delta_g$$

Our general theory connects the difference in conditional occupancy to nonequilibrium flux. Let $J(f, A)$ denote the

probability current density (horizontal arrows in Fig. 2(d)) and $\bar{J} = \int_0^1 J(f, A) df$ be the total net flux. Then, we derive in Appendix B2 [43] that

$$\text{LTGR} = \langle f \rangle \bar{g}_a + \langle 1-f \rangle \bar{g}_b + \pi_A \pi_B (\bar{T} \cdot \bar{J}) \Delta_g. \quad (13)$$

Fitness of a population is also spanned by the orthogonal coordinates of Generalism (occupancy $\langle f \rangle$) and Tracking (flux \bar{J}).

Explaining Optimal Bet Hedging: Eq. (13) generalizes the single-individual limit to the population level with temporal averages (π_a, J) replaced by spatiotemporal averages $(\langle f \rangle, \bar{J})$. Here, the cycle flux \bar{J} represents the statistical circulation of the population composition driven by environmental changes. Stochastic bet-hedging—the strategy of maintaining phenotypic diversity to avoid extinction [2]—enables this circulation to persist. When implemented via *stochastic switching* rates (w_{ab}, w_{ba}) independent of the environment, this strategy prevents natural selection from fixing the population at $f = 0$ or 1, thereby generating a continuous Tracking advantage.

This decomposition reconciles previous findings with a unified view. In the fast-growth limit, Kussell and Leibler showed that optimal switching rates match the environmental rates [4]. Our framework recovers this result (Fig. 3a) and explains the parameter-dependent deviations observed in general regimes [7]: the optimum is strictly determined by the balance between the Generalism and Tracking coordinates.

First, note that the Tracking term (proportional to \bar{J}) always forms a bell-shaped landscape in the space of stochastic switching rates (the right column in Fig. 3). This shape arises from two competing physical limits. On one hand, flux vanishes when switching rates are tiny, as the selection force ($df/dt \approx f(1-f)\Delta_{ab}$) drives the population to fixation. On the other hand, flux also vanishes when switching rates are extremely large, as rapid switching ($df/dt \approx (f_w - f)\sigma_w$) screens out the environment-dependent selection required to drive the cycle. Consequently, the Tracking advantage is maximized only at intermediate rates.

Second however, note that the total fitness is not determined by the Tracking flux alone. The Generalism term $\langle f \rangle$ creates a competing landscape. This can mask the Tracking bell shape, pushing the optimum to the boundaries (pure Generalism), as seen in Fig. 3(b). When the two environment-averaged growth rates are equal ($\bar{g}_a = \bar{g}_b$), the Generalism term becomes a flat surface (a constant \bar{g}_b). In this regime, changes in LTGR are driven solely by the Tracking coordinate. As shown in Fig. 3(c), the emergence of an optimal nonzero switching rate here is pure flux maximization, unconfounded by Generalism.

This example demonstrates the fitness parsing in a population model, explaining optimal bet-hedging as the interplay between Generalism and Tracking.

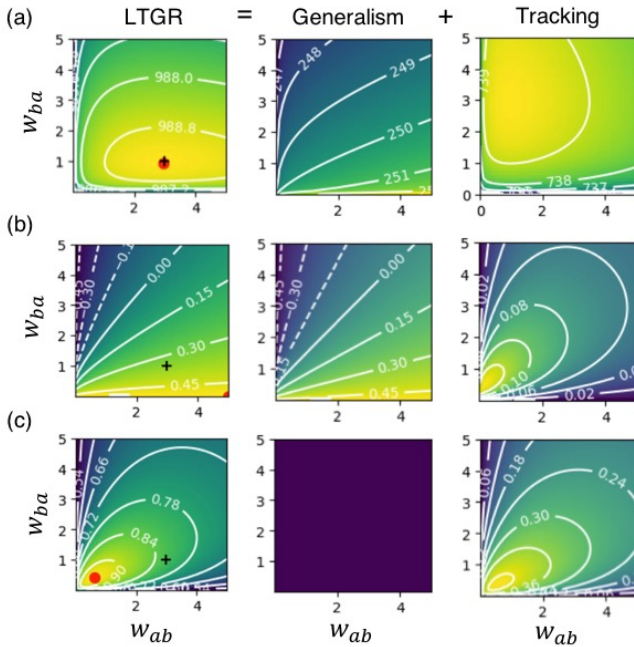


FIG. 3. **Fitness Parsing explains the existence of optimal nonzero stochastic switching rates.** Analyzing the dependence of Long-Term (logarithmic) Growth Rate (LTGR) on the stochastic switching rates (w_{ab}, w_{ba}). Black "+" denotes the position where $(w_{ab}, w_{ba}) = (R_{AB}, R_{BA})$ whereas red "o" denotes the optimal (w_{ab}, w_{ba}) . **(a) Fast growth limit.** The optimal switching rates match the environment's switching rates in this limit. **(b) When the Generalism strategy is optimal.** The case where the growth rate is not fast. The optimum LTGR happens at the boundary, with $w_{ba} = 0$. **(c) Pure Tracking / Distinct Tunability.** This is a case where the environmental average growth rates of the two types are the same: $\bar{g}_a = \bar{g}_b = 0.5$. The Generalism term becomes a flat surface, leaving the fitness landscape to be determined solely by the Tracking term. Parameters used are the following: (a) $R_{AB} = 3$, $R_{BA} = 1$, $g_a(A) = 1000$, $g_b(A) = -1000$, $g_a(B) = -1000$, $g_b(B) = 1000$; (b) $g_a(A) = 1$, $g_b(A) = -1$, $g_a(B) = -1$, $g_b(B) = 1$. All other parameters are the same as (a); (c) $R_{AB} = 3$, $R_{BA} = 1$, $g_a(A) = 5$, $g_b(A) = -1$, $g_a(B) = -1$, $g_b(B) = 1$. Parameter ranges are selected to illustrate the fast-growth limit (a) and the topological features of the fitness landscape (b,c).

EXAMPLE 3: ACHIEVING OPTIMAL PHENOTYPIC MEMORY.

Some systems can *learn and remember* something about their environments. Some microorganisms can sense their environment and switch their phenotypes accordingly, called *responsive switching* [4]. This responsive switching strategy combines the Tracking mechanisms seen in the previous two examples: the cyclic Tracking fluxes now arise from both responsive phenotype switching and differential growth. For example, *E. coli* can activate the *lac* operon to metabolize lactose when it is present, and the bacteria can turn it off when more preferred nutrients like glucose are available. Using a simple phenomenological population ODE model, Skanata and Kussell showed that there is an optimal

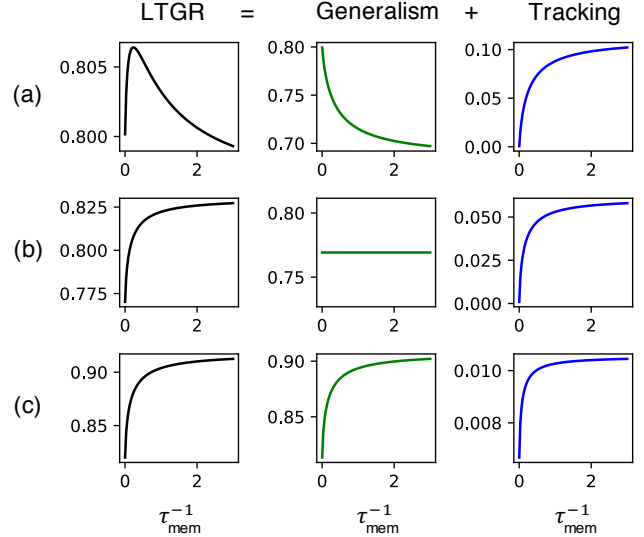


FIG. 4. **Fitness Parsing explains the existence of optimal phenotypic memory.** From (a) to (c), we increase R_{AB} from 2 to 10/3 to 10. The average growth rates of the two environments change from $(\bar{g}_a, \bar{g}_b) = (0.8, 0.6)$ to $\approx (0.769, 0.769)$ and to $= (0.72, 0.90)$. Optimal at intermediate phenotype memory cannot happen in (b) or (c) when $\bar{g}_a \leq \bar{g}_b$. Note that the y-axes for the components are individually scaled to visualize the qualitative trends in each regime. Other parameters are chosen according to the phenomenological model in [33]: fixed at $R_{BA} = 1$, $h = 1$, $\tau_{ON}^{-1} = 1$, $g = 1$, $c = 0.3$. All parameter values are chosen relative to the growth parameter g .

responsive switching rate (whose inverse is interpreted as the strength of phenotypic memory) under a stochastic switching environment [33]. Here, we show that fitness parsing can explain the mechanism behind the optimality and give the conditions for its existence.

Suppose A is the lactose environment, B is the glucose environment, a is the phenotype expressing *lac* proteins, and b is the phenotype that does not. Then, following [33] and evaluating Eq. (10a) for the two environments, the equations for the fraction f of type a under A and B are²

$$\frac{df}{dt} = f(1-f)h + (1-f)\tau_{on}^{-1}, \text{ under } A; \quad (14a)$$

$$\frac{df}{dt} = f(1-f)(-c) - f\tau_{mem}^{-1}, \text{ under } B \quad (14b)$$

where τ_{on} is the time scale to sense and reach high-level *lac* proteins, τ_{mem} is the time scale for the degradation of *lac* proteins (phenotypic memory), and the growth rates

² This phenomenological model from Skanata and Kussell assumed that the phenotype switching scheme changes perfectly with the environment, with no delay in the switching strategy changes—from $(1-f)\tau_{on}^{-1}$ to $(-f)\tau_{mem}^{-1}$ —and no back-stepping. It could be interesting to investigate how the optimality changes without these assumptions, which is beyond the scope of the current work.

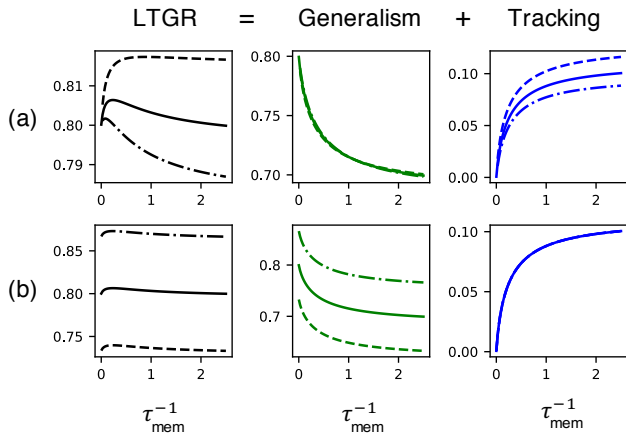


FIG. 5. **Fitness Parsing predicts the parameter dependence of fitness-memory relationship.** (a) Using the parameter set of Fig. 4(a) inherited from Ref. [33] (solid lines in this figure) as the baseline, we scale up and down the overall environmental switching rates $\theta R_{AB}, \theta R_{BA}$: $\theta = 0.8$ case shown in dash-dotted lines and $\theta = 1.2$ case in dash lines. This varies mainly the Tracking gain. (b) We perturb the growth rate under glucose, $g + \phi$: $\phi = -0.2$ shown in dash-dotted lines, and $\phi = +0.2$ in dash lines. This shifts only the Generalism gain. Strengths of parameter perturbations are chosen phenomenological for illustration.

for the LTGR computation are $g_a(A) = h$, $g_b(A) = 0$, $g_a(B) = g - c$, $g_b(B) = g$, with g being the growth rate under glucose, h being the growth rate of individuals with high *lac* proteins in the lactose environment, and c being the fitness cost for having high *lac* proteins under the glucose environment. Of interest here is how tuning the memory level τ_{mem} affects the LTGR.

Explaining the optimal phenotypic memory observed in [33]: We show that a weaker memory (larger τ_{mem}^{-1}) always increases the Tracking term by allowing the population to respond faster (the right hand side of Fig. 4). However, it also lowers the average fraction $\langle f \rangle$ of *lac*-expressing cells. The Generalism term in the fitness parsing, $\langle f \rangle \bar{g}_a + (1 - f) \bar{g}_b$, dictates whether this decrease in $\langle f \rangle$ is beneficial or detrimental. Crucially, this implies that an optimal intermediate memory can only exist if maintaining the memory phenotype is generally beneficial ($\bar{g}_a > \bar{g}_b$, Fig. 4a). In this regime, reducing memory hurts Generalism, creating the trade-off against the Tracking gain necessary for an intermediate optimal memory. Conversely, if $\bar{g}_a \leq \bar{g}_b$ (Fig. 4b-c), reducing memory is either neutral or beneficial for Generalism. With both components favoring faster switching, the trade-off vanishes, and no intermediate optimum exists.

Distinct system controllability: We give two examples of how the two components can be tuned separately. Scaling the environmental speed (Fig. 5a) stretches the Tracking curve (via the \bar{T} term) while leaving Generalism approximately invariant. In contrast, shifting the growth baseline (Fig. 5b) vertically shifts the Generalism contribution but leaves the

Tracking term invariant (as the growth difference Δ_g is fixed). This shows independent controllability of Generalism and Tracking.

EXAMPLE 4: ORTHOGONAL CONTROL OF ADAPTATION VIA ENVIRONMENTAL PROTOCOLS

So far, we have analyzed how systems optimize internal strategies given environmental statistics. Here, we address the inverse problem: designing environmental protocols to control a fixed adaptive system. We illustrate the utility of our framework using a minimal model of drug resistance.

When drugs are applied to killing populations of pathogens, such as bacteria, cancer, or viruses, the resulting selective pressure leads the organism to become drug-resistant. A sufficiently strong treatment of a drug will drive the rise of a resistant mutant, and subsequent treatment will fail. Accordingly, drug resistance can be viewed as an evolutionary game that we drug-givers are playing against the disease pathogen [56]. Drawing parallels to “integrated pest management” [57, 58], we use a toy model, similar to the one in [59], to demonstrate how evolutionary strategies can be explicitly designed to suppress resistance.

Consider a pathogen with drug-sensitive population N_S and drug-resistant population N_R . We assume that both subpopulations grow at rate g without drug and that the sensitive one reduces to $g - \delta$ when the drug is on. We also assume that switching from sensitive to resistant only happens under drug, with rate r , and re-sensitization happens only when there’s no drug, with rate s . For a large population, the dynamics can be described by ODEs:

$$\dot{N}_S = (g - \delta D) N_S - r D N_S + s(1 - D) N_R \quad (15a)$$

$$\dot{N}_R = g N_R + r D N_S - s(1 - D) N_R \quad (15b)$$

where $D = 1$ or 0 represents drug on or off. Denoting π_{on} as the time fraction of drug-on, we parse the population long-term growth rate under Markov stochastic or periodic drug on/off switching:

$$\text{LTGR} = [g - \langle 1 - f \rangle \pi_{\text{on}} \delta] + (\text{Tracking}) \quad (16)$$

Depending on the protocol, the Tracking term takes the form $\pi_{\text{on}} \pi_{\text{off}} (\bar{T} \cdot \bar{J}) \delta$ (Markov random) or $\pi_{\text{on}} \pi_{\text{off}} (\mathcal{K}_{\text{env}} \circ \bar{J}) \delta$ (periodic) [43]. Crucially, regardless of the protocol, the Tracking gain scales linearly with the environmental switching period. As in Example 3, this Tracking is driven by both differential growth (g versus $g - \delta$) and responsive switching (r versus s).

Distinct environmental controllability: This orthogonal controllability holds across different protocols (Fig. 6). **First, rapid switching minimizes Tracking.** As the cycle period vanishes ($\bar{T} \rightarrow 0$), the Tracking gain diminishes, leaving growth dominated by the Generalism baseline. This aligns with the “alternating therapy” strategy in cancer [60–62],

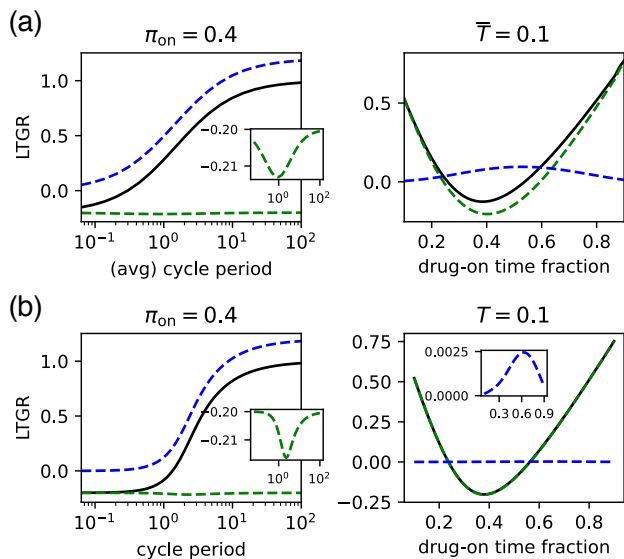


FIG. 6. **Fast environment switching reduces Tracking gain whereas optimal environment time fraction reduces Generalism gain.** (a) shows the total long-term population growth rate of drug sensitive or resistant cells under Markov random on/off drug switching. On the left, we vary the average cycle period $\bar{T} = \bar{T}_{on} + \bar{T}_{off}$ where $\bar{T}_{on/off}$ represents long-term average drug on/off intervals and fix the drug-on time fraction $\pi_{on} = \bar{T}_{on}/\bar{T}$. On the right, we vary π_{on} and fix \bar{T} . (b) is similar to (a) but under periodic environment: $T = T_{on} + T_{off}$ where $T_{on/off}$ is the fixed interval of on/off and $\pi_{on} = T_{on}/T$. Blue dashed lines are the Tracking components whereas the green dashed lines are the Generalism components. Parameters in both (a) and (b) are $g = 1, \delta = 5, r = 1, s = 3$. See Appendix C3 of SM [43] for how these are chosen. The time unit is chosen to be 100 days, i.e. rate quantities are per 100 days.

where rapid alternation of non-cross-resistant drugs is often recommended. While clinical outcomes have been mixed, showing both successes [63, 64] and failures [65–67], our framework offers a physical interpretation: efficacy hinges on minimizing the Tracking flux J driven by re-sensitization. We expect that extending this analysis—from our minimal two-state model to realistic multi-state systems—will help reconcile these disparate findings, predicting optimal protocols by identifying specific regimes where Tracking is effectively suppressed.

Second, an optimal time fraction minimizes Generalism.

Equation (16) shows that the Generalism component is minimized at an intermediate drug-on fraction π_{on} . In the limits ($\pi_{on} \rightarrow 0$ or 1), the population adapts to a static environment (growth rate g). At intermediate fractions, however, the population retains a sub-population of sensitive cells ($\langle 1 - f \rangle > 0$) while still facing frequent drug pressure ($\pi_{on} > 0$). This combination maximizes the “cost” term $(1 - f)\pi_{on}\delta$, effectively suppressing the Generalism baseline.

This analysis suggests a rational, two-pronged strategy for suppressing resistance: use **fast switching** to eliminate the

Tracking axis, and an **optimal duty cycle** (π_{on}) to minimize fitness along the Generalism axis.

DISCUSSION

Quantifying Adaptivity via Observable Coordinates.

Our framework provides a practical principle for experimental quantification: even without measuring microscopic nonequilibrium fluxes, the Tracking contribution can be computed as the residual fitness:

$$\text{Tracking} = \text{LTGR}_{\text{measured}} - \text{Generalism}(\pi_E, \pi_x). \quad (17)$$

By subtracting the calculable baseline of Generalism from the measured total growth rate, one can isolate the specific contribution of Tracking, providing a simple yet powerful metric to gauge the “nonequilibrium advantage” of systems adapting the varying environments.

Experimental Connections and Robustness. The inputs required for our analysis—such as growth rates and switching rates in the model—are standard variables that can be measured or fitted from time-series data in microfluidic and synthetic setups [13, 14]. A key strength of this framework is its robustness: while our examples explored wide parameter ranges to illustrate distinct regimes (e.g., from slow to fast switching), the predicted qualitative trends—specifically the distinct sensitivities of Tracking to time-scales and Generalism to biases—rely on the generic structure of the nonequilibrium dynamics, not on fine-tuned parameter values. This suggests that the orthogonal control strategies we propose are generic across different adaptive systems.

Cyclic Origins of Tracking. The Tracking component is sustained by nonequilibrium fluxes (J). While connecting these fluxes to precise metabolic costs requires specific energetic models, decomposing fluxes into cycles allows us to further dissect the distinct mechanisms of Tracking. As detailed in Appendix C1 [43], the cycle decomposition of fluxes [68] partitions Tracking gain based on whether the driving cycles are intrinsic to the system or involve system-environment coupling. The former represents the system’s “intrinsic nonequilibriumness,” while the latter represents the coupling. Appendix C1 shows that Tracking remains possible even when all intrinsic cycle affinities are zero [43], demonstrating that the nonequilibrium Tracking can be generated solely by system-environment coupling.

Conclusion. By mapping fitness onto the orthogonal, measurable coordinates of Generalism and Tracking, this work constructs the navigational map for the optimization and control of adaptation, determining when organisms—or engineered systems—should invest in static robustness versus dynamic responsiveness.

ACKNOWLEDGMENTS

We thank Gábor Balázs and the anonymous referees for insightful feedback and Corey Weistuch for pointing us to Ref. [59], which led us to develop the model in Example 4. We are grateful for the financial support from the Laufer Center for Physical and Quantitative Biology at Stony Brook, the John Templeton Foundation (Grant ID 62564), and NIH (Grant RM1-GM135136).

DATA AVAILABILITY STATEMENT

The codes producing the plotted data can be found at [69].

AUTHORS CONTRIBUTION

All authors conceptualized the project together. YJY developed the theory and derived the main results. CK validated and refined the results and developed the model used in Example 4. KD supervised all developments. All authors contributed equally to writing and editing the manuscript.

-
- [1] A. Murugan, K. Husain, M. J. Rust, C. Hepler, J. Bass, J. M. J. Pietsch, P. S. Swain, S. G. Jena, J. E. Toettcher, A. K. Chakraborty, K. G. Sprenger, T. Mora, A. M. Walczak, O. Rivoire, S. Wang, K. B. Wood, A. Skanata, E. Kussell, R. Ranganathan, H.-Y. Shih, and N. Goldenfeld, Roadmap on biology in time varying environments, *Phys. Biol.* **18**, 041502 (2021), publisher: IOP Publishing.
- [2] E. Levien, J. Min, J. Kondev, and A. Amir, Non-genetic variability in microbial populations: survival strategy or nuisance?, *Rep. Prog. Phys.* **84**, 116601 (2021).
- [3] J. R. Bernhardt, M. I. O'Connor, J. M. Sunday, and A. Gonzalez, Life in fluctuating environments, *Phil. Trans. R. Soc. B* **375**, 20190454 (2020).
- [4] E. Kussell and S. Leibler, Phenotypic Diversity, Population Growth, and Information in Fluctuating Environments, *Science* **309**, 2075 (2005).
- [5] D. M. Wolf, V. V. Vazirani, and A. P. Arkin, Diversity in times of adversity: probabilistic strategies in microbial survival games, *Journal of Theoretical Biology* **234**, 227 (2005).
- [6] M. C. Donaldson-Matasci, C. T. Bergstrom, and M. Lachmann, When Unreliable Cues Are Good Enough., *The American Naturalist* **182**, 313 (2013), publisher: The University of Chicago Press.
- [7] M. K. Belete and G. Balázs, Optimality and adaptation of phenotypically switching cells in fluctuating environments, *Phys. Rev. E* **92**, 062716 (2015).
- [8] B. Xue, P. Sartori, and S. Leibler, Environment-to-phenotype mapping and adaptation strategies in varying environments, *PNAS* **116**, 13847 (2019).
- [9] M. Acar, J. T. Mettetal, and A. van Oudenaarden, Stochastic switching as a survival strategy in fluctuating environments, *Nat Genet* **40**, 471 (2008), number: 4 Publisher: Nature Publishing Group.
- [10] M. E. Grantham, C. J. Antonio, B. R. O'Neil, Y. X. Zhan, and J. A. Brisson, A case for a joint strategy of diversified bet hedging and plasticity in the pea aphid wing polyphenism, *Biology Letters* **12**, 20160654 (2016), publisher: Royal Society.
- [11] J. R. Gremer, S. Kimball, and D. L. Venable, Within- and among-year germination in Sonoran Desert winter annuals: bet hedging and predictive germination in a variable environment, *Ecology Letters* **19**, 1209 (2016), _eprint: <https://onlinelibrary.wiley.com/doi/pdf/10.1111/ele.12655>.
- [12] C. S. Maxwell and P. M. Magwene, When sensing is gambling: An experimental system reveals how plasticity can generate tunable bet-hedging strategies, *Evolution* **71**, 859 (2017).
- [13] G. Lambert and E. Kussell, Memory and Fitness Optimization of Bacteria under Fluctuating Environments, *PLOS Genetics* **10**, e1004556 (2014), publisher: Public Library of Science.
- [14] D. Nevozhay, R. M. Adams, E. Van Itallie, M. R. Bennett, and G. Balázs, Mapping the Environmental Fitness Landscape of a Synthetic Gene Circuit, *PLoS Comput Biol* **8**, e1002480 (2012).
- [15] T. Saigusa, A. Tero, T. Nakagaki, and Y. Kuramoto, Amoebae anticipate periodic events, *Phys. Rev. Lett.* **100**, 018101 (2008).
- [16] I. Tagkopoulos, Y.-C. Liu, and S. Tavazoie, Predictive Behavior Within Microbial Genetic Networks, *Science* **320**, 1313 (2008), publisher: American Association for the Advancement of Science.
- [17] A. Mitchell, G. H. Romano, B. Groisman, A. Yona, E. Dekel, M. Kupiec, O. Dahan, and Y. Pilpel, Adaptive prediction of environmental changes by microorganisms, *Nature* **460**, 220 (2009).
- [18] K. Whitehead, M. Pan, K.-i. Masumura, R. Bonneau, and N. S. Baliga, Diurnally Entrained Anticipatory Behavior in Archaea, *PLOS ONE* **4**, e5485 (2009).
- [19] S. E. Marzen and J. P. Crutchfield, Optimized bacteria are environmental prediction engines, *Phys. Rev. E* **98**, 012408 (2018), publisher: American Physical Society.
- [20] M. L. Jabbur, B. P. Bratton, and C. H. Johnson, Bacteria can anticipate the seasons: Photoperiodism in cyanobacteria, *Science* **385**, 1105 (2024).
- [21] S. Wang and L. Dai, Evolving generalists in switching rugged landscapes, *PLOS Computational Biology* **15**, e1007320 (2019), publisher: Public Library of Science.
- [22] V. Sachdeva, K. Husain, J. Sheng, S. Wang, and A. Murugan, Tuning environmental timescales to evolve and maintain generalists, *Proceedings of the National Academy of Sciences* **117**, 12693 (2020).
- [23] M. Slatkin, Hedging one's evolutionary bets, *Nature* **250**, 704 (1974), publisher: Nature Publishing Group.
- [24] D. L. Venable, Bet Hedging in a Guild of Desert Annuals, *Ecology* **88**, 1086 (2007), _eprint: <https://onlinelibrary.wiley.com/doi/pdf/10.1890/06-1495>.
- [25] A. J. Grimbergen, J. Siebring, A. Solopova, and O. P. Kuipers, Microbial bet-hedging: the power of being different, *Current Opinion in Microbiology* **25**, 67 (2015).
- [26] J. Müller, B. A. Hense, T. M. Fuchs, M. Utz, and C. Pötsche, Bet-hedging in stochastically switching environments, *Journal of Theoretical Biology* **336**, 144 (2013).

- [27] A. Solopova, J. van Gestel, F. J. Weissing, H. Bachmann, B. Teusink, J. Kok, and O. P. Kuipers, Bet-hedging during bacterial diauxic shift, *Proceedings of the National Academy of Sciences* **111**, 7427 (2014), publisher: Proceedings of the National Academy of Sciences.
- [28] A. Mayer, T. Mora, O. Rivoire, and A. M. Walczak, Diversity of immune strategies explained by adaptation to pathogen statistics, *Proceedings of the National Academy of Sciences* **113**, 8630 (2016), publisher: Proceedings of the National Academy of Sciences.
- [29] P. G. Hufton, Y. T. Lin, T. Galla, and A. J. McKane, Intrinsic noise in systems with switching environments, *Phys. Rev. E* **93**, 052119 (2016).
- [30] P. G. Hufton, Y. T. Lin, and T. Galla, Phenotypic switching of populations of cells in a stochastic environment, *J. Stat. Mech.* **2018**, 023501 (2018).
- [31] L. Dinis, J. Unterberger, and D. Lacoste, Pareto-optimal trade-off for phenotypic switching of populations in a stochastic environment, *J. Stat. Mech.* **2022**, 053503 (2022), publisher: IOP Publishing and SISSA.
- [32] A. Mayer, T. Mora, O. Rivoire, and A. M. Walczak, Transitions in optimal adaptive strategies for populations in fluctuating environments, *Phys. Rev. E* **96**, 032412 (2017), publisher: American Physical Society.
- [33] A. Skanata and E. Kussell, Evolutionary Phase Transitions in Random Environments, *Phys. Rev. Lett.* **117**, 038104 (2016), publisher: American Physical Society.
- [34] P. Patra and S. Klumpp, Emergence of phenotype switching through continuous and discontinuous evolutionary transitions, *Phys. Biol.* **12**, 046004 (2015), publisher: IOP Publishing.
- [35] P. Ao, Potential in stochastic differential equations: novel construction, *J. Phys. A: Math. Gen.* **37**, L25 (2004).
- [36] J. Wang, L. Xu, and E. Wang, Potential landscape and flux framework of nonequilibrium networks: Robustness, dissipation, and coherence of biochemical oscillations, *PNAS* **105**, 12271 (2008).
- [37] Y.-J. Yang and Y.-C. Cheng, Potentials of continuous Markov processes and random perturbations, *J. Phys. A: Math. Theor.* **54**, 195001 (2021).
- [38] Y.-J. Yang and K. A. Dill, *A Principled Basis for Nonequilibrium Network Flows* (2025), arXiv:2410.17495v3 [cond-mat].
- [39] L. Van Valen, A new evolutionary law, *Evolutionary Theory* **1**, 1 (1973).
- [40] P. Ao, Laws in Darwinian evolutionary theory, *Physics of Life Reviews* **2**, 117 (2005).
- [41] F. Zhang, L. Xu, K. Zhang, E. Wang, and J. Wang, The potential and flux landscape theory of evolution, *J. Chem. Phys.* **137**, 065102 (2012), publisher: American Institute of Physics.
- [42] H. Qian, Fitness and entropy production in a cell population dynamics with epigenetic phenotype switching, *Quant Biol* **2**, 47 (2014).
- [43] See Supplementary Material at [URL] for derivations and discussions.
- [44] D. Hartich, A. C. Barato, and U. Seifert, Stochastic thermodynamics of bipartite systems: transfer entropy inequalities and a Maxwell's demon interpretation, *J. Stat. Mech.* **2014**, P02016 (2014), publisher: IOP Publishing and SISSA.
- [45] J. M. Horowitz and M. Esposito, Thermodynamics with Continuous Information Flow, *Phys. Rev. X* **4**, 031015 (2014).
- [46] M. P. Leighton, J. Ehrich, and D. A. Sivak, Information Arbitrage in Bipartite Heat Engines, *Phys. Rev. X* **14**, 041038 (2024), publisher: American Physical Society.
- [47] U. Seifert, Entropy Production along a Stochastic Trajectory and an Integral Fluctuation Theorem, *Phys. Rev. Lett.* **95**, 040602 (2005).
- [48] M. Esposito and C. Van den Broeck, Three Detailed Fluctuation Theorems, *Phys. Rev. Lett.* **104**, 10.1103/PhysRevLett.104.090601 (2010).
- [49] H. Ge and H. Qian, Physical origins of entropy production, free energy dissipation, and their mathematical representations, *Phys. Rev. E* **81**, 051133 (2010).
- [50] V. Mustonen and M. Lässig, Fitness flux and ubiquity of adaptive evolution, *PNAS* **107**, 4248 (2010).
- [51] T. J. Kobayashi and Y. Sughiyama, Fluctuation Relations of Fitness and Information in Population Dynamics, *Phys. Rev. Lett.* **115**, 238102 (2015).
- [52] A. Genthon and D. Lacoste, Fluctuation relations and fitness landscapes of growing cell populations, *Sci Rep* **10**, 11889 (2020), publisher: Nature Publishing Group.
- [53] R. Rao and S. Leibler, Evolutionary dynamics, evolutionary forces, and robustness: A nonequilibrium statistical mechanics perspective, *Proc. Natl. Acad. Sci. U.S.A.* **119**, e2112083119 (2022).
- [54] C. Maes, Frenesy: Time-symmetric dynamical activity in nonequilibria, *Physics Reports* **850**, 1 (2020).
- [55] A. C. Barato, D. Hartich, and U. Seifert, Efficiency of cellular information processing, *New J. Phys.* **16**, 103024 (2014).
- [56] A. Stein, M. Salvioli, H. Garjani, J. Dubbeldam, Y. Viossat, J. S. Brown, and K. Staňková, Stackelberg evolutionary game theory: how to manage evolving systems, *Philosophical Transactions of the Royal Society B* **378**, 20210495 (2023).
- [57] C. J. Whelan and J. J. Cunningham, Resistance is not the end: lessons from pest management, *Cancer Control* **27**, 1073274820922543 (2020), publisher: SAGE Publications Inc.
- [58] R. A. Gatenby and J. S. Brown, Integrating evolutionary dynamics into cancer therapy, *Nature reviews Clinical oncology* **17**, 675 (2020).
- [59] M. Robertson-Tessi, J. S. Brown, M. I. Poole, M. Johnson, A. Marusyk, J. A. Gallaher, K. A. Luddy, C. J. Whelan, J. West, M. Strobl, V. Turati, H. Enderling, M. J. Schell, A. Tan, T. Boyle, R. Mankanji, J. Farinhas, H. Soliman, D. Lemanne, R. A. Gatenby, D. R. Reed, A. R. A. Anderson, and C. H. Chung, *Feasibility of an Evolutionary Tumor Board for Generating Novel Personalized Therapeutic Strategies* (2023), pages: 2023.01.18.23284628.
- [60] J. Goldie, A. Coldman, and G. Gudauskas, Rationale for the use of alternating non-cross-resistant chemotherapy, *Cancer Treat Rep* **66**, 439 (1982).
- [61] M. Strobl, J. Gallaher, M. Robertson-Tessi, J. West, and A. Anderson, Treatment of evolving cancers will require dynamic decision support, *Annals of Oncology* **34**, 867 (2023).
- [62] M. Perry, D. Doll, and C. Freter, *Perry's The Chemotherapy Source Book* (Wolters Kluwer Health, 2012).
- [63] J. H. Glick, M. L. Young, D. Harrington, R. L. Schilsky, T. Beck, R. Neiman, R. I. Fisher, B. A. Peterson, and M. M. Oken, Mopp/abv hybrid chemotherapy for advanced hodgkin's disease significantly improves failure-free and overall survival: the 8-year results of the intergroup trial., *Journal of clinical oncology* **16**, 19 (1998).
- [64] H. E. Grier, M. D. Krailo, N. J. Tarbell, M. P. Link, C. J. Fryer, D. J. Pritchard, M. C. Gebhardt, P. S. Dickman, E. J. Perlman, P. A. Meyers, *et al.*, Addition of ifosfamide and etoposide to standard chemotherapy for ewing's sarcoma and primitive neuroectodermal tumor of bone, *New England Journal of Medicine* **348**, 694 (2003).

- [65] G. Bonadonna, M. Zambetti, and P. Valagussa, Sequential or alternating doxorubicin and cmf regimens in breast cancer with more than three positive nodes: ten-year results, *Jama* **273**, 542 (1995).
- [66] J. Aisner, C. Cirrincione, M. Perloff, M. Perry, D. Budman, J. Abrams, L. Panasci, H. Muss, M. Citron, and J. Holland, Combination chemotherapy for metastatic or recurrent carcinoma of the breast—a randomized phase iii trial comparing caf versus vath versus vath alternating with cmfvp: Cancer and leukemia group b study 8281., *Journal of clinical oncology* **13**, 1443 (1995).
- [67] S. De Placido, F. Perrone, C. Carlomagno, A. Morabito, C. Pagliarulo, R. Lauria, A. Marinelli, M. De Laurentiis, E. Varriale, G. Petrella, *et al.*, Cmf vs alternating cmf/ev in the adjuvant treatment of operable breast cancer. a single centre randomised clinical trial (naples gun-3 study), *British journal of cancer* **71**, 1283 (1995).
- [68] D.-Q. Jiang, M. Qian, and M.-P. Qian, *Mathematical Theory of Nonequilibrium Steady States: On the Frontier of Probability and Dynamical Systems*, 2004th ed. (Springer, Berlin ; New York, 2004).
- [69] See DOI: 10.5281/zenodo.15733979 for the Source Codes performing the numerical calculations and plotting the Figures.